EUROfusion

WPMAT-PR(17) 18129

MJ Caturla et al.

Insights from atomistic models on loop nucleation and growth in ?-Fe thin films under Fe + 100 keV irradiation

Preprint of Paper to be submitted for publication in
Acta Materialia

This work has been carried out within the framework of the EUROfusion Consortium and has received funding from the Euratom research and training programme 2014-2018 under grant agreement No 633053. The views and opinions expressed herein do not necessarily reflect those of the European Commission.

Insights from atomistic models on loop nucleation and growth in α-Fe thin films under Fe^+ 100 keV irradiation

J. P. Balbuena[a], M. J. Aliaga[a], I. Dopico[b], M. Hernández-Mayoral[c], L. Malerba[d], I. Martin-Bragado[e], M. J. Caturla[a1]

[A] Dep. Física Aplicada, Universidad de Alicante, E-03690 Spain
[b] Universidad Politécnica de Madrid, ETS de Ingenieros de Caminos, 28040 Madrid
[c] CIEMAT, Madrid, Spain
[d] SCK-CEN, Belgium
[e] UCAM, Universidad Católica de Murcia, Campus de los Jerónimos 3017, Guadalupe, Murcia

Abstract

The question of loop growth in a-Fe under irradiation is addressed using object kinetic Monte Carlo with parameters from molecular dynamics and density functional theory calculations. Two models are considered for the formation of <100> loops, both based on recent atomistic simulations. In one model <100> loops are formed by the interaction between ½ <111> loops. In a second model small interstitial clusters, nucleated in the collision cascade, can grow as <100> or ½ <111> loops. Comparing results from the two models to experimental measurements of loop densities, ratios and sizes produced by Fe 100 keV irradiation of Fe thin films, the validity of the models is addressed.

Keywords: Monte Carlo simulation, Ion irradiation, Iron, Irradiation effect, In situ transmission electron microscopy.

1. Introduction

An outstanding question in the field of radiation damage effects in Fe-based alloys is the nucleation and growth of loops under irradiation. Experimentally, it is well known since the 1960s that two types of loops are formed: <100> and 1/2<111> loops [1-7]. However, the character (vacancy or self-interstitial), concentration, ratio and sizes of these loops differs considerably depending on the experimental conditions. Moreover, the reason why these loops are observed is still not completely clear. Elasticity theory and simulations predict that ½<111> loops have lower energies than <100> loops and should be the dominant defect at low temperatures [8, 9]. As temperature increases, <100> loops become more stable due to the magnetic transition that iron experiences at 770°C [10]. On the other hand ½<111> loops are highly mobile according to computer simulations [11-13] in what could be considered as an athermal migration [14]. Therefore,

1Corresponding author.
E-mail address: mj.caturla@ua.es Phone number: +34 965903400 ext.2056

these clusters should quickly migrate to sinks such as dislocations, grain boundaries or surfaces and not be observed in the bulk.

Several explanations have been given within the past few years for the presence of both <100> and ½<111> loops, coming from computer simulations as well as detailed experimental measurements. The observation of ½<111> loops despite their fast migration is explained by the presence of traps, that slow down the motion of these clusters. Experiments performed by Arakawa et al. [15] have shown that the migration energy of these loops is closer to 1 eV than to the 0.1 eV values obtained from atomistic simulations [11-13]. Several candidates have been proposed as the possible traps for these clusters [16-19]. Carbon, that is always present even if in very low concentrations, could affect the mobility of these loops [16-17]. This interaction could be aided by vacancies, forming C-vacancy complexes that can then trap self-interstitial loops [18, 19]. The interaction of these loops among themselves could also form junctions that make them immobile [16].

The presence of <100> loops has been more difficult to elucidate and it is still an open question. There are currently two main explanations, both based on computer simulations. Marian et al [20] proposed the formation of these loops from reactions between ½<111> loops, supported by molecular dynamics (MD) simulations and based on the earlier work of Masters [1]. Later on, Xu et al. [21] observed the formation of these loops by reactions between ½ <111> using MD together with advanced kinetic Monte Carlo calculations. In this later work, the formation of <100> loops through these reactions was clearly obtained from the simulations. More recently, a new possible mechanism of formation of these loops has been proposed based on the work of Marinica et al [22]: <100> loops could grow from small immobile clusters, C15 clusters [23].

Microstructure evolution in irradiated Fe has been simulated with kinetic Monte Carlo and rate theory models by several groups [16, 19, 24-26]. However, except for a recent work by Terentyev and Martin-Bragado for electron irradiation [19], no distinction is made for self-interstitial clusters, and the ratios between <100> and ½<111> loops are not followed. In this work, we have gather the existing information about cluster stabilities and mobilities together with the different models for growth of loops in Fe explained above. All these parameters and reactions have been implemented in a kinetic Monte Carlo model and have been used to model irradiation at low energies, 100keV, in Fe thin films. The results obtained in terms of defect densities and sizes from the two different models for loop growth have been contrasted with experimental measurements [6].

Yao et al [6] performed a series of systematic studies of irradiation of thin films of Fe and Fe-Cr alloys with heavy ions, with in-situ transmission electron microscopy (TEM) analysis. Fe^{+} and Xe^{+} ions of energies of 100 keV and 150 keV were used for irradiations both at room temperature and 300°C. Loops were first observed at doses above 10^{16} m^{-2} and both <100> and ½<111> loops could be identified, with a much higher proportion of <100> specially for Fe foils. Foil orientation had an important effect in Fe films but not in Fe-Cr samples. In this work we focus on

the results for room temperature and Fe samples irradiated with 100 keV Fe^+ ions. The comparison between experiments and simulations allows us to extract some conclusions about the most probable mechanism for loop growth under these irradiation conditions.

2. Model parametrization

We have used our database of 100 keV cascades of Fe irradiation of Fe thin films [27] as input for the Object Kinetic Monte Carlo code MMonCa, developed by I. Martin-Bragado [28]. The simulation box we have used is also a thin film of 50nm, reproducing a typical TEM sample. Box sizes for parametric studies were 200x200x50 nm^3 and for comparison with experiments larger boxes were used to increase statistics: 400x400x50 nm^3. In our code, small self-interstitial atom (SIA) clusters up to size 4 have irregular shape and are considered mobile, with the migration energies given in table I obtained from density functional theory (DFT) calculations [29]. These self-interstitial clusters are considered to move in three dimensions. From size 5, they can grow according to one of this two models:

“Reaction” model: In this model all interstitial clusters above size 4 transform into 1/2<111> loops with mobilities given also in table I and obtained from classical molecular dynamics simulations [13]. These loops move one-dimensionally, unlike vacancies or smaller SIA clusters. The interaction between <111> loops results in the formation of <100> loops, <111> + <111> = <100> when the size of the two <111> loops is similar, that is, when the difference between the sizes of the two loops is less than 5% of the loop size, and when both clusters are above a size threshold of 15 SIAs, as suggested by the simulations of Marian et al. [20]. The minimum size of ½<111> loops to form <100> clusters is one of the parameters that has been evaluated in this work. Once the <100> loops are formed, they can grow by addition of small interstitial clusters (≤ 4).

“Nucleation” model: In this model <111> and <100> loops form and grow independently. SIA clusters from size 5 can either transform into <100> loops or into <111> loops with a given ratio. This ratio was initially taken as 5%, following the idea of the Marinica et al [22] that considers this as the ratio of C15 clusters formed in a collision cascade, and assuming that all these clusters will grow into <100> loops. The influence of this ratio has also been evaluated as discussed in the next section. Once formed, both types of loops can grow by addition of small self-interstitial clusters (≤ 4).

In both models 1/2<111> loops can be stopped by the interaction with carbon and carbon-vacancy and carbon-interstitial clusters following the work of Terentyev and Martin-Bragado [19]. These immobile C-<111> loops can then grow by addition of SIA clusters < 5. In the case of model A, they can also grow by addition of mobile ½<111> loops. Also, <100> vacancy loops have been included in the models. The equation derived by Gilbert in [30] has been used for the binding energy of the vacancies in the loop. In this equation the radius of the loop is calculated using the size and the density of the loop. The density of the

loop has been calculated fitting the equation to figure 4 in [30]. For the binding energies of $V_n > 4$ and $I_n>4$ clusters, we have used the usual extrapolation law [31]: $E_b(n)=E_f+[E_b(2)-E_f][n^{2/3}-(n-1)^{2/3}]/(2^{2/3}-1)$. For the smaller species up to 4 DFT values have been used [29]. These small vacancy clusters are considered mobile, with a 3D mobility, while larger vacancy clusters are immobile. Table 1 summarizes the most important parameters of the species involved.

Table 1: Type of defect, migration and binding energies of the objects defined in our OKMC model. Last column corresponds to the dimensionality of migration. For the mono-defects, V and I, the formation energy is taken from ab initio calculations [29], $E_f(V)=2.07$ eV and $E_f(I)=3.77$ eV.

Defect	Migration Barrier (eV)	Binding energies (eV)	Migration type
V	0.67		3D
V2	0.62	0.3	3D
V3	0.35	0.37	3D
V4	0.48	0.62	3D
Vn > 4	immobile	As in ref. [Son98]	
V 100 loops	0.5	As in ref. [Gil08]	
I	0.34		3D
I2	0.42	0.8	3D
I3	0.43	0.92	3D
I4	0.3	1.64	3D
In>4, I111 loops	0.06+0.11/n1.6	As in ref. [Soneda98]	1D
In > 4, I100 loops	Immobile	As in ref. [Soneda98]	
C-I111 loops	Immobile	1.3	

One specific feature of MMonCa is that the location of all defects in a cluster are explicitly defined. This allows for more flexibility for the capture volume of a defect since it is not restricted to a sphere, but it is given by the shape of the cluster defined by the defects that form that cluster. The interaction between two clusters will then happen when the distance between two defects belonging to each cluster is smaller or equal than the specified capture radius. In this case the capture radius used is equal to the jump distance, first nearest neighbors in Fe: 0.287 nm.

As mentioned above, the database used for these simulation has been obtained from molecular dynamics simulations with the specific experimental conditions: 100 keV Fe irradiation of Fe [27]. Those simulations showed that the damage distribution obtained from this particular irradiation energy is very different from that in the case of bulk irradiation. Particularly, <100> vacancy loops with more than 400 defects were obtained. These loops are always located within a few layers from the surface. In principle, <100> loops have a low mobility. However, if

we consider that all <100> vacancy loops formed in the MD simulations do not migrate or recombine with the surface, the concentration of <100> loops is extremely high and in complete disagreement with the experimental observations Therefore, these <100> vacancy loops must migrate or recombine with the surface. We have used in the OKMC simulations a migration energy of 0.5 eV in both models. MD simulations of vacancy loops close to the surface are being performed to study this issue.

The conditions for the irradiation follow those in the experiment by Yao et al. [6]. Simulations are performed at room temperature, with a dose rate of $8x10^{14}$ ions/m^2/s in pure Fe and Fe with different carbon concentrations. Foil orientations along (100) and (111) are studied. The concentration of defects as a function of dose is analyzed under different conditions of foil orientation, carbon concentration as well as the type of model for loop growth, the reaction and the nucleation model, as explained above. In order to compare with experimental measurements of defect densities obtained by TEM it is important to take into account the minimum visible size resolvable experimentally. This is considered in our simulations as clusters having 100 defects or more, value corresponding to a cluster of a diameter of ~1.5 nm [32] and used before by different authors [16, 24, 26].

3. Results

Figure 1a shows the concentration of visible defects as a function of irradiation dose obtained from the two models for loop growth described above. In these simulations no carbon was included, therefore, due to the fast migration of ½<111> loops to the surface, all remaining loops are of <100> type. The minimum size considered for ½<111> loops to form <100> loops in the reaction model is 15, while the ratio of <100> to ½<111> loops in the nucleation model is 5%. The main difference that can be observed in figure 1a is that in case of the reaction model, when <100> loops are formed by interaction between ½<111> loops, visible clusters are formed at very early doses with concentrations as high as 10^{14} m^{-2} for a dose of $2x10^{16}$ ions/m^2. The dependence with dose is significantly different for the case of the nucleation model, that is, when <100> loops grow from small clusters within the collision cascade. In this case, visible defects appear at much higher doses and the raise with dose is steeper than in the case of the reaction model. The difference between the two models can also be seen in figure 1b where the defect size distribution is presented for a dose of $3.2x10^{17}$ ions/m^2. For the reaction model less than 10% of the clusters have a diameter of 2 nm or less, while a large fraction have sizes between 2 and 4 nm. In the nucleation model, most of the clusters have diameters of 2 nm or less. The maximum cluster size in the nucleation model is 4 nm while in the reaction model clusters can be as large as 6 nm. Note that we are considering cascade damage where defect clusters are already formed. Figures 1c and 1d show the location of the loops in the simulation box across the thickness of the film for the reaction and nucleation model respectively and for a dose of $3.2x10^{17}$ ions/m^2. This is similar to what would be observed under TEM, except that here loops of all sizes

are shown, and not only visible ones. The difference between the two models is clearly seen in these figures.

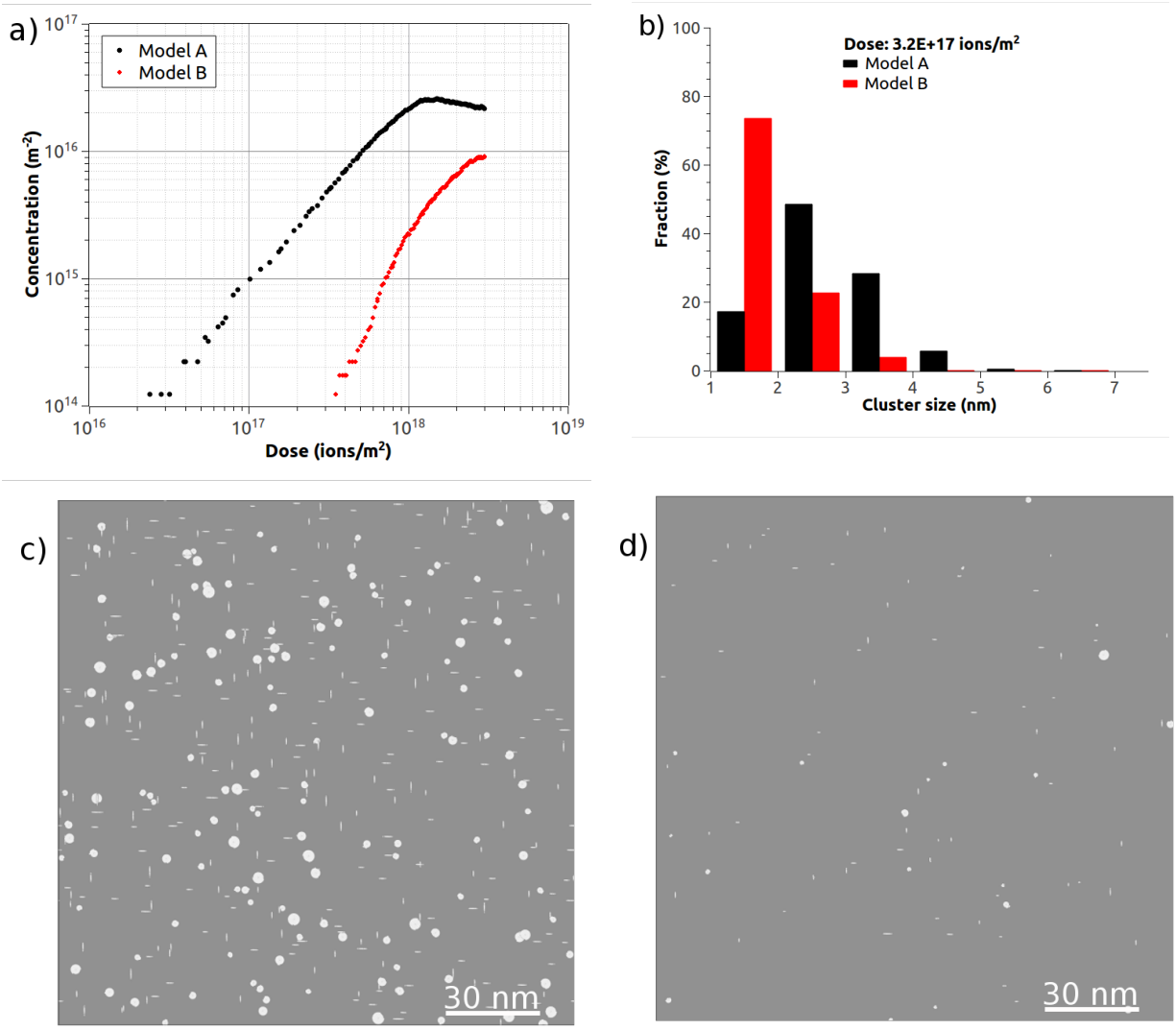

Figure 1: *Comparison between the two loop growth models (a) Total concentration of visible clusters as a function of irradiation dose (b) Cluster size distribution for a dose of 3.2x10^{17} ions/m^2. The distribution of loops at this dose within the thin film are shown in (c) for the reaction model and (d) for the nucleation model.*

Both models have one parameter that could change the outcome of the evolution of defects. In the case of the reaction model this parameter is the size at which the ½<111> loops can react to form a <100> loop. According to the work of Marian [20] as well as the work of Xu [21], in order to form a <100> loop the reacting clusters must have similar sizes. Marian [20] also states that loops must have at least 15 defects each in order to form a <100> loop. We have performed

calculations for different sizes of the ½<111> loops that would give rise to the formation of a <100>, presented in figure 2a for minimum sizes between 30 and 90 self-interstitials (or 15 and 45 self-interstitials on each interacting loop). This figure shows that as the minimum size for loop formation increases, the concentration of <100> loops decreases. However, the trend of concentration with dose remains the same, independently of the value of this parameter. It is also interesting to note that at low doses, there is no significant difference up to a minimum size of 90 defects. This is due to the fact that self-interstitial clusters of more than 50 defects can be already formed in the collision cascade, therefore providing the nucleation seed for these visible <100> loops from very early on.

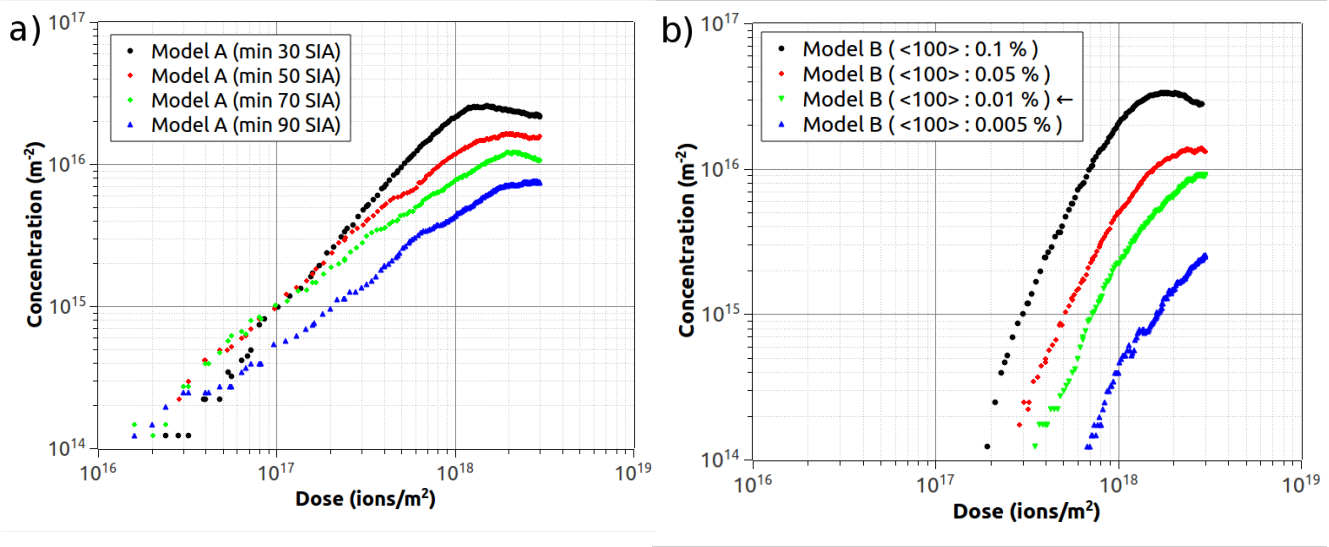

Figure 2: *Dependence of the reaction models and the nucleation model on their respective parameter for <100> loop nucleation (a) Reaction model, minimum size of ½<111> loops to form <100> (b) Nucleation model, ratio between ½<111> and <100> loops within the collision cascade. The arrow in the nucleation model indicates the parameter that gives better agreement with the experimental measurements.*

In the case of the nucleation model, the parameter that controls the concentration of <100> loops is the ratio of <100> and ½<111> loops considered to be formed within the collision cascade. According to the work of Marinica [22] about 5% of all clusters produced in a collision cascade are of type C15. However, not necessarily all these clusters are going to evolve to <100> loops. Figure 2b shows the dependence of visible cluster concentration on the percentage of clusters considered to be <100> loops. As expected, the total concentration decreases as the percentage decreases, without any significant change in the dose dependence. As mentioned above, experimentally visible

clusters are only observed for doses above 10^{16} m^{-2}. For the case of pure Fe, concentrations are below 10^{15} m^{-2} for the highest doses studied. Note that in the reaction model, these concentrations are reached even at a dose as low as 10^{17} m^{-2} . In the nucleation model, visible clusters are observable at higher doses. In fact, the best agreement with the experimental results is obtained for the case where a ratio of <100> to ½<111> loops is only 0.01%, as we will show below.

In these simulations, only <100> loops remain in the thin film, due to the recombination of the 1D migrating ½<111> loops with the surfaces. Experimentally, however, even in the ultra-high pure Fe samples, both ½<111> and <100> loops are observed with a much higher concentration of <100> (86%). This is in contradiction to the results presented in figures 1 and 2. One possible explanation, as discussed in the introduction, is the trapping of self-interstitial loops by carbon. Therefore, we have considered different carbon concentrations. Figure 3 shows the results for the case of the nucleation model including carbon with a ratio of 0.01% <100>to ½<111>. Figure 3a presents the visible concentration of <100> and ½<111> loops as a function of dose as well as the total concentration for 100 appm carbon. Now both types of loops are present, with higher concentration of <100> loops (~62%). Figure 3b presents the total concentration of visible clusters as a function of dose for different carbon concentrations from no carbon up to 1000 appm.

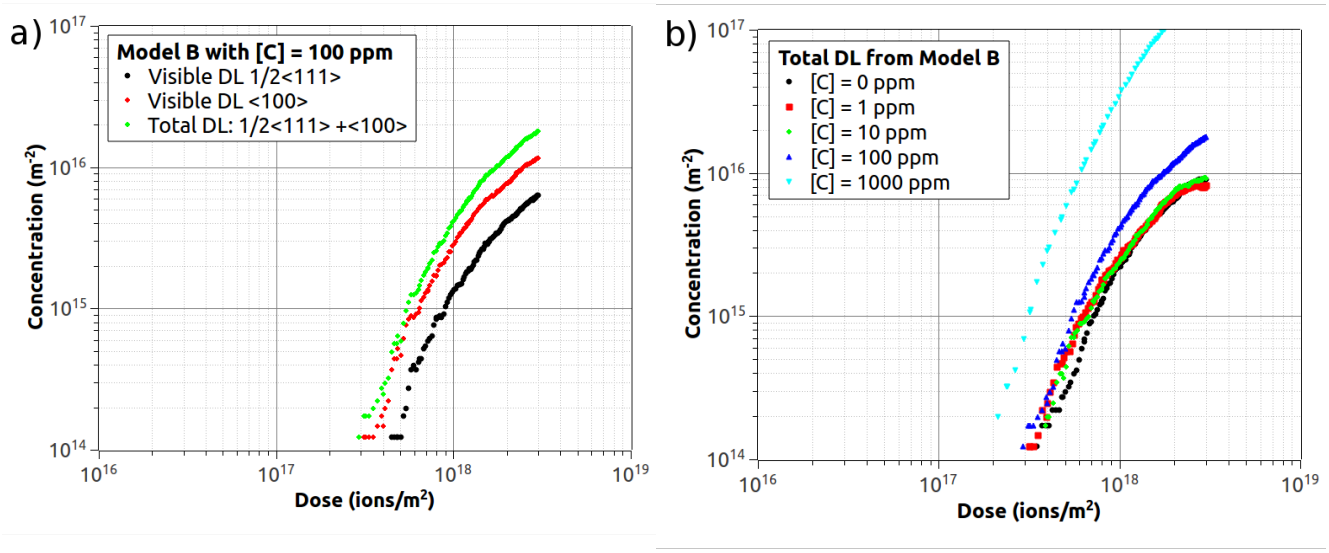

Figure 3: *Nucleation model including carbon as traps for ½ <111> loops. (a) Total visible clusters together with <100> and ½<111> loops for 100 appm carbon concentration (b) Total visible clusters for different carbon concentrations.*

Note that there are no significant differences in the total concentration for carbon concentrations between 0 and 10 appm, but the ratio of <100> vs ½<111> loops changes depending on the carbon concentration. Figure 4 shows the fraction of <100> loops as a function of carbon concentration for the highest doses simulated here, $3x10^{18}$ ions/m^2. Note that the ratio of <100>/<111> loops changes very rapidly after a concentration of 10 appm. For a carbon concentration of about 50 appm, about 90% of the loops would be of <100> type, according to this model, which would be close to the value measured experimentally.

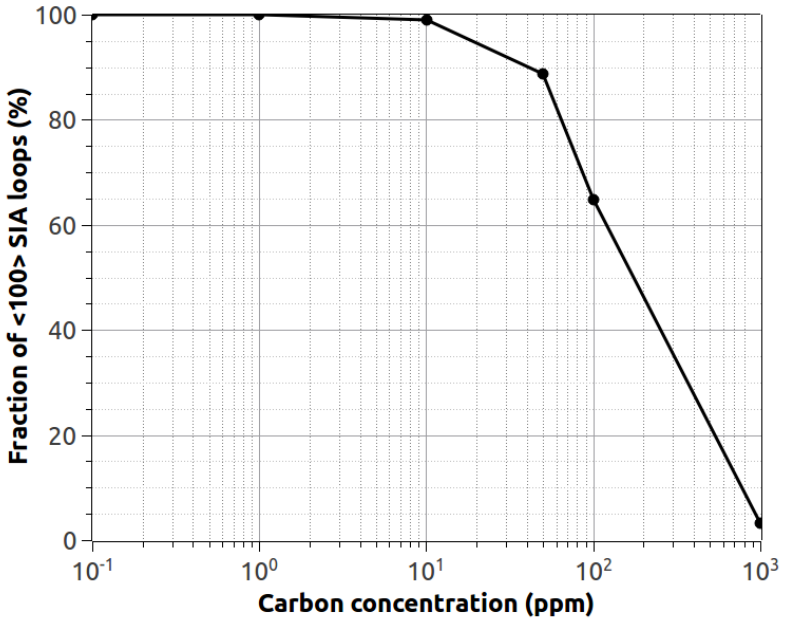

Figure 4: *Ratio of <100> loops as a function of carbon concentration for the highest simulated dose, $3x10^{18}$ ions/m^2.*

4. Discussion

From the analysis above, the results obtained with the nucleation model seem to give the best fit to the experimental observations. Figure 5 shows a comparison of the visible cluster concentration as a function of dose for the two models together with the experimental measurements. The parameters for the simulations are those that optimize the comparison to the experiment, that is, minimum size for <100> loop formation of 90 defects for the reaction model and a ratio of 0.01% for the transformation of small SIA clusters to <100> loops for the nucleation model. In both cases the carbon concentration is 50 appm. Two sets of experimental results are included, those for polycrystalline Fe analyzed on a (111) orientation and one point obtained for single crystal with a (100) orientation. As already pointed out earlier, the reaction model overestimates the concentration of defects at low doses. This fast growth of visible clusters is even more evident when carbon is included in the simulation, since ½<111> loops trapped in carbon

sites can rapidly grow by the coalescence with other ½<111> loops. Consequently, the formation of visible clusters occurs from the early doses since clusters are already formed in the collision cascade, which can coalesce and quickly grow into visible clusters. This is significantly different from electron irradiation, where isolated Frenkel pairs are formed. The results from the nucleation model give a much better agreement with the experimental measurements, as can be seen in figure 5a. The general trend in terms of concentration as a function of dose with this model reproduces very well the experimental results.

Calculations for two different crystal orientations (100) and (111) have also been performed, presented in figure 5. Although there is a slight difference between the two orientations, with lower concentrations for (111) orientation, in agreement with the experimental results, this difference is much smaller than that observed experimentally. This result seems to indicate that the interaction of the mobile interstitials with the surface should be stronger than what has been considered in the model. Currently defects interact with the surface only when they are located within a distance equal to a jump distance, 0.287 nm. However, due to image forces [33] the interaction of the surface with loops could be a much longer range which would enhance recombination in particular in the (111) orientation. Molecular dynamics simulations are currently being performed to test this hypothesis.

Figure 5b shows the distribution of loops across the thin film for the nucleation model at a dose of 3.2×10^{17} ions/m^2 . White disks are <100> loops while dark ones are ½<111>. Defects of all sizes are shown here. This figure clearly shows that, although the concentration of visible <100> loops is higher than that of ½<111>, there is a high population of the later, trapped at carbon. This could reverse the population of visible loops at higher doses as observed experimentally [7]. The evolution of the loop size can also be seen in the histograms presented in figure 5c and 5d, for two different doses.

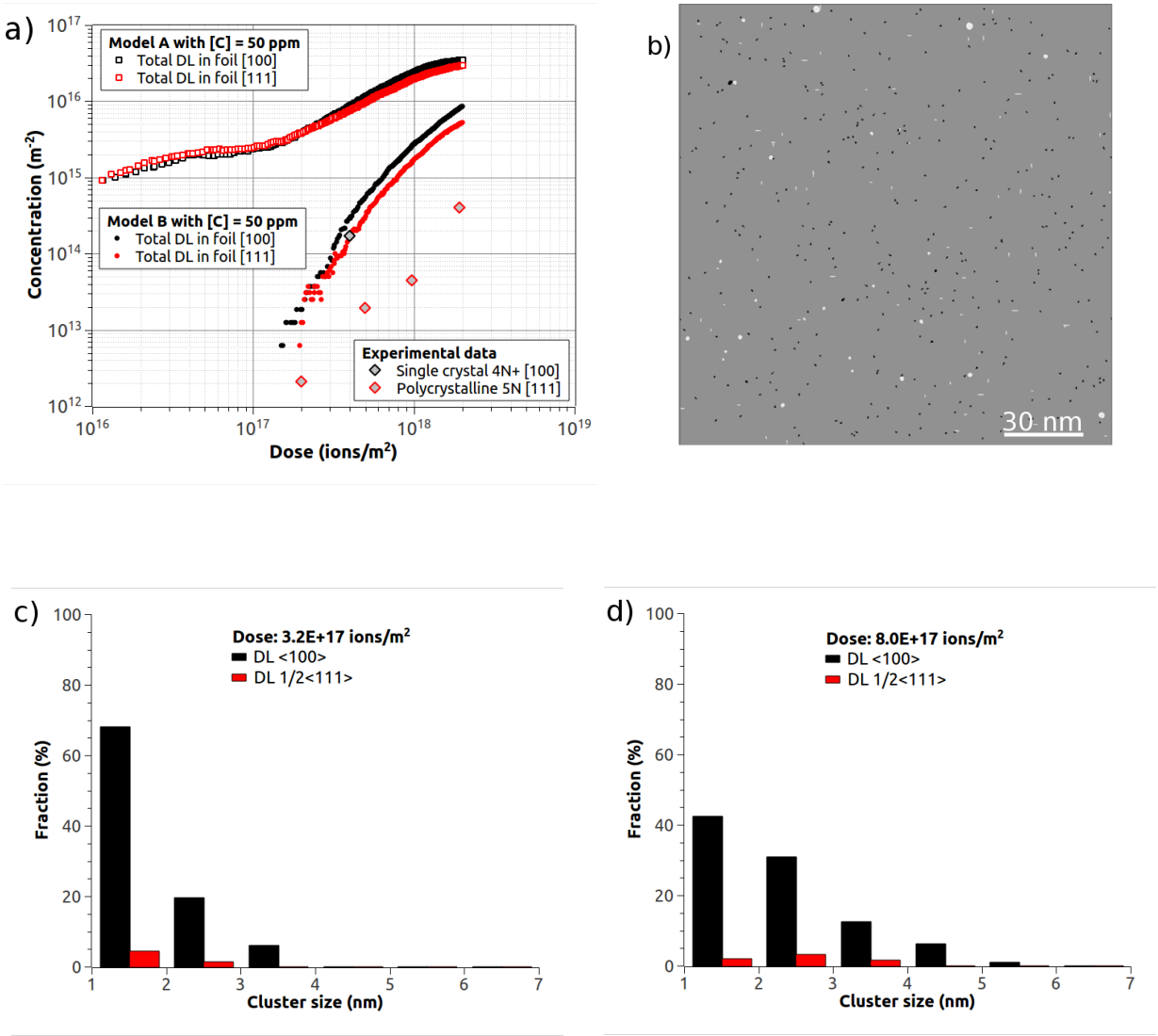

Figure 5: *Comparison of the two models with experimental data from Yao et al [6] (a) Total visible clusters as a function of dose (lines) compared to experimental measurements (symbols) for two different crystal orientations (b) Image of loops across the thickness of the film for the nucleation model at a dose of 3.2x10^{17} ions/m^2 and (100) crystal orientation. White disks are <100> loops while dark ones are ½ <111> loops. (c) and (d) Cluster size distribution also for the nucleation model and two doses.*

5. Conclusions

Through kinetic Monte Carlo simulations and parameters obtained both from classical molecular dynamics simulations and density functional theory, we have studied two growth models for self-interstitial loops in alpha-Fe. The models have been contrasted to TEM characterizations of Fe 100 keV irradiation of Fe thin films. From this comparison we conclude that a model that considers <100> loops generated within the collision cascade (or from small clusters in the collision cascade such as C15) is more plausible than a model where <100> loops are formed as the coalescence of ½<111> loops. The later model gives rise to visible loops at low doses since self-interstitial clusters are already formed within the collision cascade. This results in a dependence of defect concentration with dose that does not match the experimental evidence.

We should point out, however, that this could be a consequence of the particular experimental conditions considered in this work. Experiments were performed in thin films and consequently surfaces play a strong role in microstructure evolution. What these simulations indicate is that, under these conditions, the interaction of surfaces with mobile ½<111> loops should be stronger than the interaction between loops. However, in bulk irradiation conditions, such as high energy ion implantation (MeV) or neutron irradiation, the mechanism of interactions between loops to produce <100> clusters can not be disregarded.

Acknowledgements

This work has been carried out within the framework of the EUROfusion Consortium and has received funding from the Euratom research and training programme 2014-2018 under grant agreement No 633053. The views and Opinions expressed herein do not necessarily reflect those of the European Commission. The research leading to these results is partly funded by the European Atomic Energy Community's (Euratom) Seventh Framework Programme FP7/2007-2013 under grant agreement No. 604862 (MatISSE project) and in the framework of the EERA (European Energy Research Alliance) Joint Programme on Nuclear Materials.

Bibliography

[1] B.C. Masters, Dislocation loops in irradiated iron, Nature 200 (1963) 254.
[2] M.L. Jenkins, C.A. English, B.L. Eyre, Heavy-ion damage in alpha Fe, Nature 263 (1976) 400–401.
[3] B.L. Eyre, Transmission electron microscopy studies of point defect clusters in fcc and bcc metals J. Phys. F: Metal Phys. 3, 422 (1973).
[4] B.L. Eyre, Proc. Conf. Defects in Refractory Metals, SCK-CEN, Mol, p. 311 (1973).
[5] E. A. Little, R. Bullough, and M. H. Wood, On the swelling resistance of ferritic steels. Proceedings of the Royal Society of London Series a-Mathematical Physical and Engineering Sciences **372**, 565 (1980).
[6] Z. Yao, M. Hernández Mayoral, M.L. Jenkins, M.A. Kirk, Heavy-ion irradiations of Fe and Fe–Cr model alloys Part 1: Damage evolution in thin-foils at lower doses, Philos. Mag. 88 (2008) 2851.
[7] M. Hernández-Mayoral, Z. Yao, M.L. Jenkins, M.A. Kirk, Heavy-ion irradiations of Fe and Fe–Cr model alloys Part 2: Damage evolution in thin-foils at higher doses, Philos. Mag. 88 (2008) 2881.
[8] B. Evre and R. Bullough, On the formation of interstitial loops in bcc metals. Philosophical Magazine **12**, 31 (1965).
[9] R. Bullough, in *15th Anniversary of the Concept of Dislocation in Crystals* (The Institute of Metals, London, 1984), p. 283.
[10] S. L. Dudarev, R. Bullough, and P. M. Derlet, Effect of the α−γ Phase Transition on the Stability of Dislocation Loops in bcc Iron. Physical Review Letters 100 (2008) 135503.
[11] D. J. Bacon, F. Gao, Y. N. Osetsky, The primary damage state in fcc, bcc and hcp metals as seen in molecular dynamics simulations. J. Nucl. Mater. 276 (2000) 1
[12] B. D. Wirth, G. R. Odette, D. Maroudas, G. E. Lucas, Dislocation loop structure, energy and mobility of self-interstitial atom clusters in bcc iron. J. Nucl. Mater. 276 (2000) 33
[13] N. Soneda, T. Diaz de la Rubia, Migration kinetics of the self-interstitial atom and its clusters in bcc Fe. Phil. Mag. A 81 (2001) 331.
[14] S. Dudarev, The non-Arrhenius migration of interstitial defects in bcc transition metals. C.R.Physique **9**, 409 (2008)
[15] K. Arakawa, K. Ono, M. Isshiki, K. Mimura, M. Uchikoshi, and H. Mori, Observation of the One-Dimensional Diffusion of Nanometer-Sized Dislocation Loops. Science 318, 956 (2007)
[16] M. J. Caturla, N. Soneda, E. Alonso, B. D. Wirth, T. Diaz de la Rubia, J. M. Perlado, Comparative study of radiation damage accumulation in Cu and Fe, J. of Nucl. Mat. 276 (2000) 13
[17] Y. Satoh, H. Matsui, and T. Hamaoka, Effects of impurities on one-dimensional migration of interstitial clusters in iron under electron irradiation, Phys. Rev. B 77 (2008), p. 094135.

[18] N. Anento and A. Serra,Carbon–vacancy complexes as traps for self-interstitial clusters in Fe–C alloys. Journal of Nuclear Materials 440 (2013) 236–242.
[19] D. Terentyev, I. Martin-Bragado, Evolution of dislocation loops in iron under irradiation: The impact of carbon. Scripta Materialia 97 (2015) 5-8.
[20] J. Marian, B. D. Wirth, J. M. Perlado, Mechanism of Formation and Growth of ⟨100⟩ Interstitial Loops in Ferritic Materials. Phys. Rev. Lett. 88 (2002) 255507
[21] H. Xu, R. E. Stoller, Y. N. Osetsky, D. Terentyev, Solving the Puzzle of ⟨100⟩ Interstitial Loop Formation in bcc Iron. Phys. Rev. Lett. 110 (2013) 265503
[22] M.-C. Marinica, F. Willaime, J.-P. Crocombette, Irradiation-Induced Formation of Nanocrystallites with C15 Laves Phase Structure in bcc Iron, Phys. Rev. Lett. 108 (2012) 025501
[23] Y. Zhang, X.-M. Bai, M. R. Tonks, A. B. Biner. Formation of prismatic loops from C15 Laves phase interstitial clusters in body-centered cubic iron. Scripta Materialia 98 (2015) 5-8.
[24] C. Domain, C. S. Becquart, L. Malerba, Simulation of radiation damage in Fe alloys: an object kinetic Monte Carlo approach. J. Nucl. Mater. 335 (2004) 121
[25] A. Hardouin Dupartc, C. Moingeon, N. Smetniansky-de-Grande, A. Barbu, Microstructure modelling of ferritic alloys under high flux 1 MeV electron irradiations. J. Nucl. Mater. 302 (2002) 143
[26] V. Jansson, M. Chiapetto, L. Malerba, The nanostructure evolution in Fe–C systems under irradiation at 560 K. J. of Nucl. Mat. 442 (2013) 341
[27] M. J. Aliaga,R. Schäublin, J. F. Löffler, M. J. Caturla, Surface-induced vacancy loops and damage dispersion in irradiated Fe thin films. Acta Mat. 101 (2015) 22
[28] I. Martin-Bragado, A. Rivera, G. Valles, J. L. Gomez-Selles, M. J. Caturla, MMonCa: An Object Kinetic Monte Carlo simulator for damage irradiation evolution and defect diffusion. Computer Physics Comm. 184 (2013) 2703; MMonCa. <http://www.materials.imdea.org/MMonCa>
[29] C. C. Fu, J. Dalla Torre, F. Willaime, J.-L. Bouquet, A. Barbu, Multiscale modelling of defect kinetics in irradiated iron. Nature Materials 4 (2005) 68.
[30] M R Gilbert, S. L. Dudarev, P. M. Derlet, D. G. Pettifor. Structure and metastability of mesoscopic vacancy and interstitial loop defects in iron and tungsten. J. Phys.: Condens. Matter 20 (2008) 345214.
[31] N. Soneda and T. Díaz de la Rubia, Defect production, annealing kinetics and damage evolution in α-Fe: An atomic-scale computer simulation. Phil. Mag. A 78, (1998) 995-1019
[32] Loop visibility threshold, clusters with more than 100 defects.
[33] A. Prokhodtseva, B. Décamps, R. Schäublin, Comparison between bulk and thin foil ion irradiation of ultra high purity Fe, J. Nucl. Mater. 442 (2013) S786–S789.